Continuous Monitoring of Sonomyography, Electromyography and Torque Generated by Normal Upper Arm Muscles During Isometric Contraction: Sonomyography Assessment for Arm Muscles

Jun Shi, Yong-Ping Zheng*, *Senior Member, IEEE*, Qing-Hua Huang, *Member, IEEE*, and Xin Chen

***Abstract*—The aim of this study is to demonstrate the feasibility of using the continuous signals about the thickness and pennation angle changes of muscles detected in real-time from ultrasound images, named as sonomyography (SMG), to characterize muscles under isometric contraction, along with synchronized surface electromyography (EMG) and generated torque signals. The right biceps brachii muscles of seven normal young adult subjects were tested. We observed that exponential functions could well represent the relationships between the normalized EMG root-mean-square (RMS) and the torque, the RMS and the muscle deformation SMG, and the RMS and the pennation angle SMG for the data of the contraction phase, with exponent coefficients of 0.0341 ± 0.0148 (Mean $\pm$ SD), 0.0619 ± 0.0273, and 0.0266 ± 0.0076, respectively. In addition, the preliminary results also demonstrated linear relationships between the normalized torque and the muscle deformation as well as the pennation angle with the ratios of 9.79 ± 3.01 and 2.02 ± 0.53, respectively. The overall mean R^2 for the regressions was approximately 0.9 and the overall mean relative root mean square error (RRMSE) smaller than 15%. The potential values of SMG together with EMG to provide a more comprehensive assessment for the muscle functions should be further investigated with more subjects and more muscle groups.**

***Index Terms*—Electromyography, EMG, muscle, pennation angle, SMG, sonomyography, ultrasound.**

I. Introduction

ULTRASOUND and surface electromyography (EMG) are two of the most commonly used approaches for the assessment of skeletal muscles in vivo and can provide muscle architectural and electrophysiological features, respectively. Many studies have been previously reported on the relationships between the surface EMG and muscle force [1], [2], length [2], and action-potential conduction velocity [3]–[5], etc. On the other hand, sonography, i.e., ultrasound imaging, has been widely used to assess human muscles in both static and dynamic conditions. In recent years, sonography has been employed to measure the changes in muscle thickness [6]–[8], fiber pennation angle [9]–[13], fascicle length [6], [9]–[13], dimension [14], and cross-sectional area [9], [15] during isometric and dynamic contractions. Since these architectural parameters change obviously with contraction, they could potentially provide a noninvasive method of recording activities from deep muscles without the complication of the cross-talk from adjacent muscles suffered in the EMG analysis [7]. More recently, some studies have been reported on the relationship between the EMG activity and the muscle architectural parameters extracted from sonography in quasi-static ways [7], [13], [16], [17]. It has been demonstrated in literature that the architectural and EMG parameters can provide complementary information for muscle assessment. However, few study reported continuous collection of ultrasound, EMG and other parameters simultaneously in real-time. EMG signals were usually sampled firstly under a certain muscle contraction level, and ultrasound images were then collected at the same condition, but not simultaneously. Some recent studies have reported the continuous monitoring of EMG and ultrasound images of muscles [13], but the two data streams were independently collected and the data analysis and synchronization had to be performed off-line. Ultrasound has also been used to measure muscle stiffness changes during isometric contraction by monitoring the change of sound speed in the muscle, earlier *in vitro* [18], [19] and recently *in vivo* [20]. Since the muscle stiffness change is directly related to its deformation, the stiffness monitoring techniques show potentials for the muscle assessment. However, current *in vivo* stiffness measurement techniques cannot provide continuous measurement yet.

The aim of this study is to demonstrate the feasibility of continuous monitoring of muscle thickness and pennation angle changes under isometric contractions using real-time ultrasound images. These real-time changes of muscle architectures were named as sonomyography (SMG), and they were used to evaluate muscle contractions together with synchronized surface electromyography (EMG) and generated torque signals. We continuously collected sonography, torque, and EMG signals simultaneously from the right biceps brachii during the flexion of the elbow from seven young adult subjects. The correlations among different signals were studied.

Manuscript received August 18, 2006; revised June 30, 2007. This work was supported in part by the Research Grants Council of Hong Kong (PolyU 5245/03E, PolyU 5331/06E), The Hong Kong Polytechnic University (G-U064, G-YE22), Shanghai Leading Academic Discipline Project (T0102) and the Development Foundation of Shanghai Education Committee (05AZ49). *Asterisk indicates corresponding author.*

J. Shi is with the Department of Health Technology and Informatics, The Hong Kong Polytechnic University, Hong Kong, and also with the School of Communication and Information Engineering, Shanghai University, Shanghai, China.

*Y.-P. Zheng is with the Department of Health Technology and Informatics, The Hong Kong Polytechnic University, Hung Hom, Kowloon, Hong Kong SAR, China (e-mail: ypzheng@ieee.org).

Q.-H. Huang and X. Chen are with the Department of Health Technology and Informatics, The Hong Kong Polytechnic University, Hong Kong.

Digital Object Identifier 10.1109/TBME.2007.909538

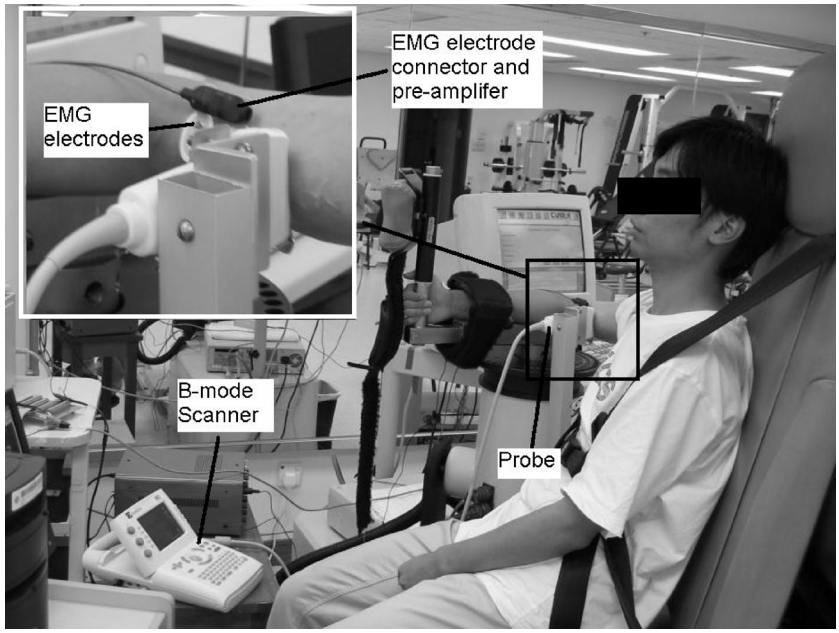

Fig. 1. Experimental setup for the measurement of muscle isometric contraction with ultrasound imaging and EMG. The area labeled with the small rectangle is magnified in the upper-left corner.

II. Methods

A. Subjects

Seven healthy male subjects participated to this study (age:27 ± 2 years; height:172 ± 4 cm; weight:65 ± 6 kg). None of them had any history of neuromuscular disorder and each gave written informed consent prior to the experiment.

B. Experimental Protocol

The subject was seated comfortably in the adjustable chair of a Cybex machine (Cybex Norm Testing & Rehabilitation System, Cybex Norm Int. Inc., Ronkonkoma, USA) with his trunk fixed by a strap onto the chair back to stabilize the posture during the test. The forearm was placed and fixed on a holder and the hand was connected to grip a vertical lever arm. The upper arm and forearm were kept in a horizontal plane parallel to ground floor. The elbow was flexed at 90° and the upper arm kept perpendicular to the trunk. The axis of the lever arm was mounted to be parallel to the rotational axis of the elbow joint. The hand maintained in the halfway between pronation and supination. The right arm was chosen for the measurement, which was the dominant one for all subjects. Fig. 1 shows the experimental setup.

After several familiarization contractions with a mild strength, the subject was asked to perform an elbow flexion against the lever arm and to increase the contraction gradually to the maximal contraction within approximately 5 s and then to relax gradually. We found that the subject could contract the muscles smoothly using this contraction rate and the muscle deformation could be successfully detected using the ultrasound images. All the subjects were instructed to follow the same contraction rate. The increase of the contraction was indicated by the increase of the torque, which was shown on the PC screen and could be monitored by the subject and the operator during the experiment. Three repeated voluntary contractions were performed continuously within each trial and totally three trials were performed with a rest of 5 min after each trial. The maximal torque value recorded during each trial was considered as the maximal voluntary contractions (MVC), which was used for the normalization for the data of this trial.

C. Data Acquisition

A dynamometer (Cybex Norm Testing & Rehabilitation System, Cybex Norm Int. Inc., Ronkonkoma, USA) was used to measure the elbow flexion torques. The torque signal from the dynamometer was amplified by a custom-made amplifier and digitized by a data acquisition card (NI PCI-6024E, National Instruments, Austin, USA) installed in the PC, where it was synchronized with the ultrasound images and EMG signals using a custom-designed program.

The sonography of the cross-sectional area of the biceps brachii was recorded using a portable B-mode ultrasound scanner (180 Plus, Sonosite Inc., Washington, USA) with a 7.5 MHz 38 mm linear probe (L38, Sonosite Inc., Washington, USA). The probe was fixed using a custom-made bracket. It was perpendicular to the skin surface of the biceps brachii region and its image plane was arranged vertically to the orientation of the biceps brachii muscle. To detect the brachialis pennation angle, another test was conducted with the probe arranged parallel to the long axis of the biceps brachii and near the elbow joint. There was a gap between the probe surface and the skin surface to avoid any compression on the tissue during the whole muscle contraction period. Hence, the change of the muscle thickness was only due to muscle contraction. The gap was filled with ultrasound gel to maintain acoustic coupling during the test. An operator took in charge of adding gel into the gap if necessary during the test, in order to maintain the acoustic coupling. The video output of B-mode ultrasound scanner was

digitized by a video capturing card (NI PCI-1411, National Instruments, Austin, USA) with a rate of 8 frames per second. The images were saved frame by frame and synchronized with other signals for subsequent analysis.

After cleaning the skin with alcohol, a pair of EMG bipolar Ag-Agcl electrodes (Axon Systems, Inc., New York, USA) was placed between the transducer and the elbow joint and along the orientation of the biceps brachii muscle. The distance between the two electrodes was 20 mm. The EMG reference electrode was placed on the proximal head of the ulna. The EMG signal was amplified and filtered by a custom-made device with a gain of 10 and bandwidth of 10–800 Hz before being digitized by the A/D card (NI PCI-6024E National Instruments, Austin, USA), and an additional gain of 10 was provided by the data acquisition card. The sample rate for EMG data collection was 4 kHz, which allowed us to collect the full bandwidth of EMG signals and has been widely used in the literature. From the spectrum analysis of the EMG signals using FFT, the adopted sampling rate appeared appropriate.

The data acquisition was controlled by the custom-developed software for the ultrasonic measurement of motion and elasticity (UMME) developed using Microsoft Visual C++ 6.0. Multithread technology was applied in UMME software to insure the synchronization among the ultrasound image, torque, and EMG. Ultrasound images were sampled frame by frame, and each frame was accompanied by an EMG epoch of 125 ms and a torque value. Each epoch of EMG contained 500 data points. The temporal calibration between the data streams of ultrasound images and other analog signals were achieved by moving the ultrasound probe in a water tank [21]. The positional change of the ultrasound probe also caused the alteration of the analog signals. The time lags between the analog signals and the signal representing the probe positional change, obtained by tracking the position of the water tank bottom in the ultrasound images, were calculated using cross-correlation matching and used for the temporal matching for the image frames and signal data points.

D. Data Analysis

All the ultrasound, EMG and torque signals were viewed on the same screen during data collection and processed off-line with the UMME software and another program written in MATLAB (Version 6.5, MathWorks, Inc., Massachusetts, USA). The root mean square (RMS) of the EMG amplitude was calculated for each epoch, containing 500 data points, using the MATLAB program. The ultrasound images were imported to UMME software and replayed frame by frame to measure muscle thickness and fiber pennation angle.

Among all kinds of image tracking algorithms, the correlation tracking has some advantages, including the tolerance for low signal noise ratio and the ability to track targets with complex structures and backgrounds [18], [23]. The cross-correlation tracking algorithm acquires a reference image or template from the previous frame and looks for the most similar area to the reference image or template for estimating the object position in the current frame [18], [24]. Two rectangular region-of-interest (ROI) were selected along the upper and lower boundaries of the biceps brachii manually in the first image

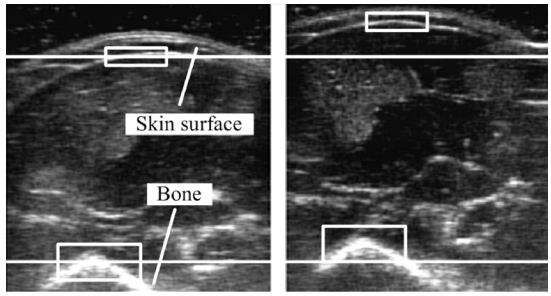

Fig. 2. Motion tracking for the ultrasound images using a two-dimensional cross-correlation algorithm. (a) The image taken at the moment before contraction and (b) the image taken when the torque reached MVC. Two rectangular ROIs were selected on the upper and lower boundaries of the cross-sectional image of biceps brachii, respectively.

frame (Fig. 2), and the pixels in these two ROIs were regarded as two templates, which were individually tracked during the muscle contraction. Because the biceps brachii is attached to the humerus, we selected the surface of humerus as the lower boundaries of biceps brachii. The criteria for selecting the locations of the rectangular ROIs were that they should be placed at the regions with the most clearly visualized upper and lower boundaries in the image and their centers were located at approximately the highest points of the upper and lower boundaries, respectively (Fig. 2). Fig. 2(a) was taken at the moment before contraction and Fig. 2(b) at the moment reaching the MVC.

The image tracking algorithm based on the 2D cross-correlation was implemented in UMME software to track the movement of each selected rectangular ROI frame by frame in both vertical and horizontal directions [8]. The best matching position was where the cross-correlation coefficient (R) reached the maximum value. When finishing matching for the current frame, the templates were updated by the pixels in the rectangular ROIs which were in the new positions. Thus the templates only needed to be manually set in the first frame and the tracking would run down till the last frame automatically. The displacements of the two tracking rectangular ROIs were continuously obtained through this process. The distance between the centers of the two ROIs was calculated for each frame, which represented the muscle thickness measured in each frame. The percentage deformation of the muscle dimension was defined as

$$\rho = \frac{d - d_0}{d_0} \times 100\% \tag{1}$$

where d_0 is the initial muscle thickness, and d is the muscle thickness of each frame.

The brachialis pennation angle α was calculated as the angle between the humeral surface and the most clearly visualized fascicle [7], which was shown in Fig. 3. Fig. 3(a) was taken at the moment before contraction and Fig. 3(b) was at the moment reaching the MVC. The reliability of the pennation angle measurement using this approach has been previously demonstrated to be high [25]. The percentage change of the pennation angle was defined as

$$\beta = \frac{\alpha - \alpha_0}{\alpha_0} \times 100\% \tag{2}$$

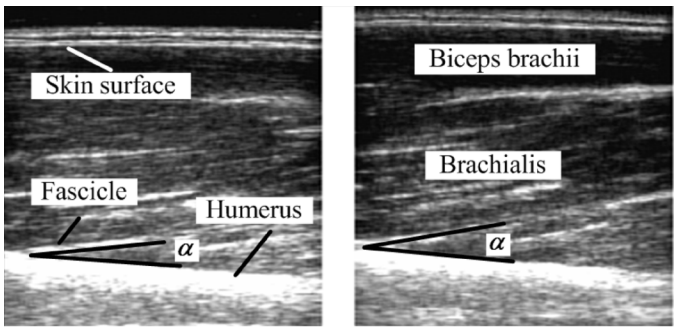

(a) (b)

Fig. 3. Pennation angle of brachialis in ultrasound images. The angle between two black lines is the pennation angle. (a) The image taken at the moment before contraction and (b) the image taken when the torque reached MVC.

where α_0 is the initial pennation angle, and α is the pennation angle measured in each frame.

The correlations among the torque, EMG RMS, muscle deformation, and pennation angle change were investigated using different regression methods. Each contraction-relaxation cycle of each trial was analyzed individually. Only the data of the contraction phases were analyzed for all the tests, as it was reported that the muscle contraction was difficult to control during the relaxation phase [7]. For each trial, the torque was normalized by its value at MVC, the EMG RMS normalized by its value at MVC, and the muscle deformation normalized by the initial muscle thickness. Two-factor ANOVA was used to test the significance of the differences of the results obtained among different trials and among different subjects. The two factors were the subject and contraction trail and were arranged as the row and column factors, respectively. Each subject-trial pair contained the parameters extracted from three repeated cycles. In order to evaluate the result of the regression between parameters, the square of the correlation coefficient (R^2) and the relative root mean square error (RRMSE) were calculated for each regression. The RRMSE is defined as follows [26]:

$$\mathrm{RRMSE} = \sqrt{\frac{\sum_i (y(i) - \hat{y(i)})^2}{\sum_i (y(i))^2}} \tag{3}$$

where $y(i)$ represents the measured values of the parameter, and $\hat{y(i)}$ are the calculated values using the selected regression. The R^2 and RRMSE values of individual subjects and their means were reported.

III. Results

A. Relationships Among Torque, EMG RMS, and Muscle Deformation

Fig. 4(a) shows a typical data set of the normalized torque and EMG RMS for one subject. The corresponding relationship between the torque and RMS data in the contraction phase is shown in Fig. 4(b). The results of other subjects showed similar trends. The observed nonlinear relationship between the torque and the RMS of EMG was consistent with the results previously reported [27], [28]. It was found that an exponential function

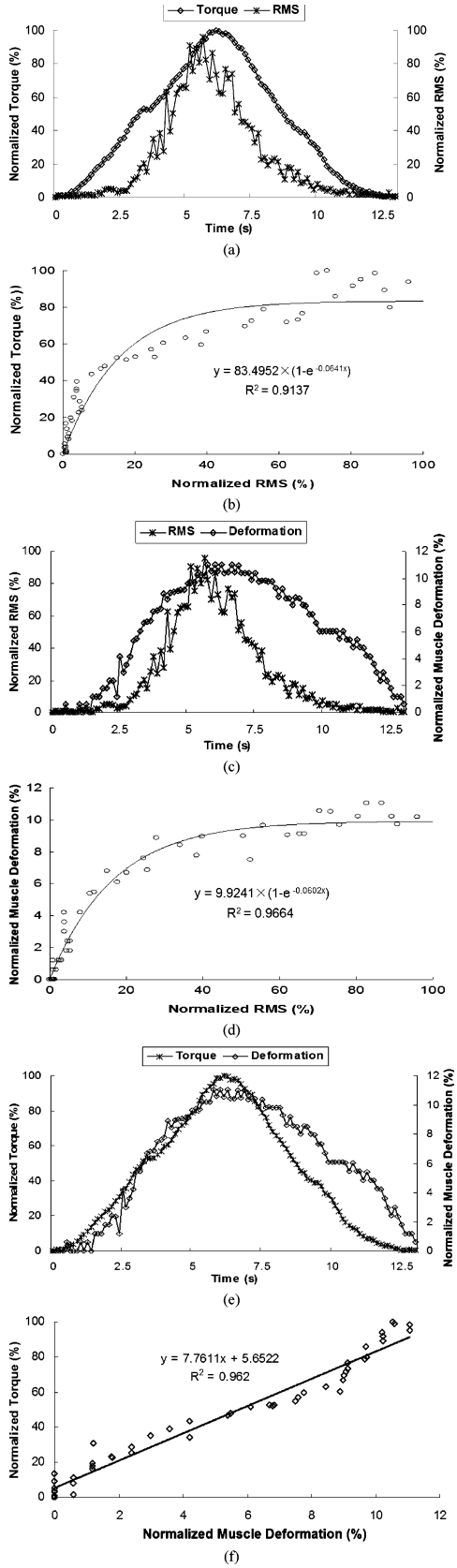

Fig. 4. Typical relationships between the normalized torque, EMG RMS and muscle deformation during one cycle of contraction process. (a) The torque and RMS signals. (b) Exponential regression between the torque and RMS. (c) The muscle deformation and RMS. (d) The exponential regression between the muscle deformation and RMS. (e) Torque and muscle deformation. (f) The linear regression between the torque and muscle deformation.

TABLE I
SUMMARY OF THE COEFFICIENTS OF THE REGRESSIONS AMONG THE TORQUE, EMG RMS, MUSCLE DEFORMATION, AND PENNATION ANGLE

Subject	A	B	C	D	E	F	G	Mean
Exponent coefficient between RMS and torque ($\times 10^{-2}$)	5.94± 1.04	3.90± 0.91.	2.09± 0.44	2.19± 0.52	1.98± 0.59	3.17± 0.55	4.55± 0.76	3.41± 1.48
Exponent coefficient between RMS and muscle deformation ($\times 10^{-2}$)	9.17± 2.43	8.93± 2.71	4.56± 1.81	3.40± 1.01	2.85± 0.73	5.64± 0.99	8.78± 3.26	6.19± 2.73
Ratio between torque and muscle deformation	8.49 ±3.85	11.98 ±2.77	12.41 ±4.15	13.43 ±3.83	7.93 ±2.35	4.89 ±1.33	9.37 ±2.50	9.79 ±3.01
Exponent coefficient between RMS and pennation change ($\times 10^{-2}$)	3.52± 0.73	3.28± 0.66	1.20± 0.35	2.50± 0.39	2.44± 0.62	3.12± 0.54	2.56± 0.46	2.66± 0.76
Ratio between torque and pennation Angle change	1.44± 0.20	1.64± 0.32	1.79± 0.48	1.86± 0.36	1.84± 0.31	2.83± 0.53	2.71± 0.32	2.02± 0.53

shown in (4) could well represent the relationship between the normalized torque and EMG RMS.

$$Y = a(1 - e^{-bX}) \tag{4}$$

where Y is the normalized torque, X is the normalized RMS value, a is the asymptotic value of Y when X is large enough, and the exponent coefficient b determines the curvature of the relationship. The constants a and b were determined with Sigmaplot software (SPSS Science, Chicago, Illinois).

Fig. 4(c) and (d) show the relationship of the EMG RMS and the muscle deformation for the same test as shown in Fig. 4(a). Exponential relationships between the EMG RMS and the muscle deformation were observed in the results of all the subjects. This finding was consistent with the results previously reported [7]. Equation (4) was used for the regressions, where the variable Y represented the normalized muscle deformation. It was found that the relationship between the torque and the muscle deformation could be well represented by a linear regression, which is shown in Fig. 4(e) and (f).

Table I summarizes the results of the regressions among the normalized torque, muscle deformation, and EMG RMS of different subjects. The means of exponent coefficients of the exponential regressions between the RMS and the torque and between the muscle deformation and the RMS were 0.0341 ± 0.0148 (Mean $\pm$ SD) and 0.0619 ± 0.0273, respectively. The mean ratio of the linear regression between the torque and muscle deformation was 9.79 ± 3.01. Two-factor ANOVA demonstrated that there were significant ($p < 0.001$) differences in the exponent coefficient of the exponential regressions and in the ratio of the linear regressions among the seven subjects but not among the three trials ($p > 0.05$). The mean R^2 and RRMSE values of the regressions between the torque and RMS, between the muscle deformation and RMS, and between the torque and muscle deformation were 0.905 ± 0.082 and $11.9\% \pm 5.1\%$, 0.880 ± 0.084 and $14.2\% \pm 6.1\%$, and 0.869 ± 0.048 and $12.6\% \pm 3.4\%$, respectively.

B. Relationships Among Pennation Angle, EMG RMS, and Torque

It was found that the relationship between the pennation angle change and the EMG RMS was obviously nonlinear [Fig. 5(a) and (b)], while that between the pennation angle and the torque was linear [Fig. 5(c) and (d)]. The results of all subjects showed similar trends. Using the exponential function shown in (5) to represent the relationship between the EMG RMS and the pennation angle, the overall mean of the exponent coefficients of the correlation was 0.0266 ± 0.0076 (Table I). Using linear regressions, the mean ratio between the torque and the pennation angle change was 2.02 ± 0.53. The mean R^2 and RRMSE values of the exponential and linear regressions were 0.904 ± 0.069 and $13.4\% \pm 4.6\%$, and 0.947 ± 0.021 and $9.8\% \pm 2.1\%$, respectively. Two-factor ANOVA did not demonstrate a significant difference of both parameters among the 3 trials ($p > 0.05$). A significant ($p < 0.001$) difference was demonstrated for the ratio of the linear regression among the 7 subjects, but not for the exponent coefficient ($p > 0.05$).

IV. DISCUSSION

In this paper, we described a method to simultaneously collect the EMG signals, torque and ultrasound images of the biceps brachii muscle during the continuous isometric contraction. The real-time architectural changes of the muscle including the muscle deformation and pennation angle were detected from ultrasound images and these signals were named as sonomyography (SMG). The results of the contraction phase showed exponential relationships between the normalized EMG RMS and the normalized torque, the normalized RMS and the muscle deformation SMG, and the RMS and the pennation angle SMG. There were linear relationships between the torque and muscle deformation as well as between the torque and pennation angle.

We have not analyzed the data for the relaxation phase of the contraction cycle in this study. It was noted that the subjects could easily increase the torque gradually to the MVC within 5 s during the contraction phase, but could not reduce the torque smoothly. This made the data of torque reducing phases having complicated patterns and difficult to analyze. In spite of that, we observed some interesting phenomena in the data of the full contraction cycle, including the hysteresis in the curves of torque-deformation, EMG RMS-deformation, torque-pennation angle, EMG RMS-pennation angle relationships. To allow subjects conducting smooth torque reducing, we should use a higher contraction-relaxation rate. However, this is limited by the relatively low frame rate (8 Hz) of the present system. By testing gastrocnemius muscles invasively, Orizio *et al.* [29] reported the hysteresis of the curve between the muscle force and deformation, which was measured using a laser distance sensor. They also reported that the muscle deformation rate tended to be lower during the relaxation phase in comparison with that in the contraction phase. Similar phenomenon was observed in our study, such as the results shown Fig. 4(e), though it had not been obtained from all the subjects due to the reason explained above. Future studies using higher frame rate are required to investigate temporal relationships among the signals of muscle deformation, pennation angle change, and EMG RMS under different muscle contraction rates.

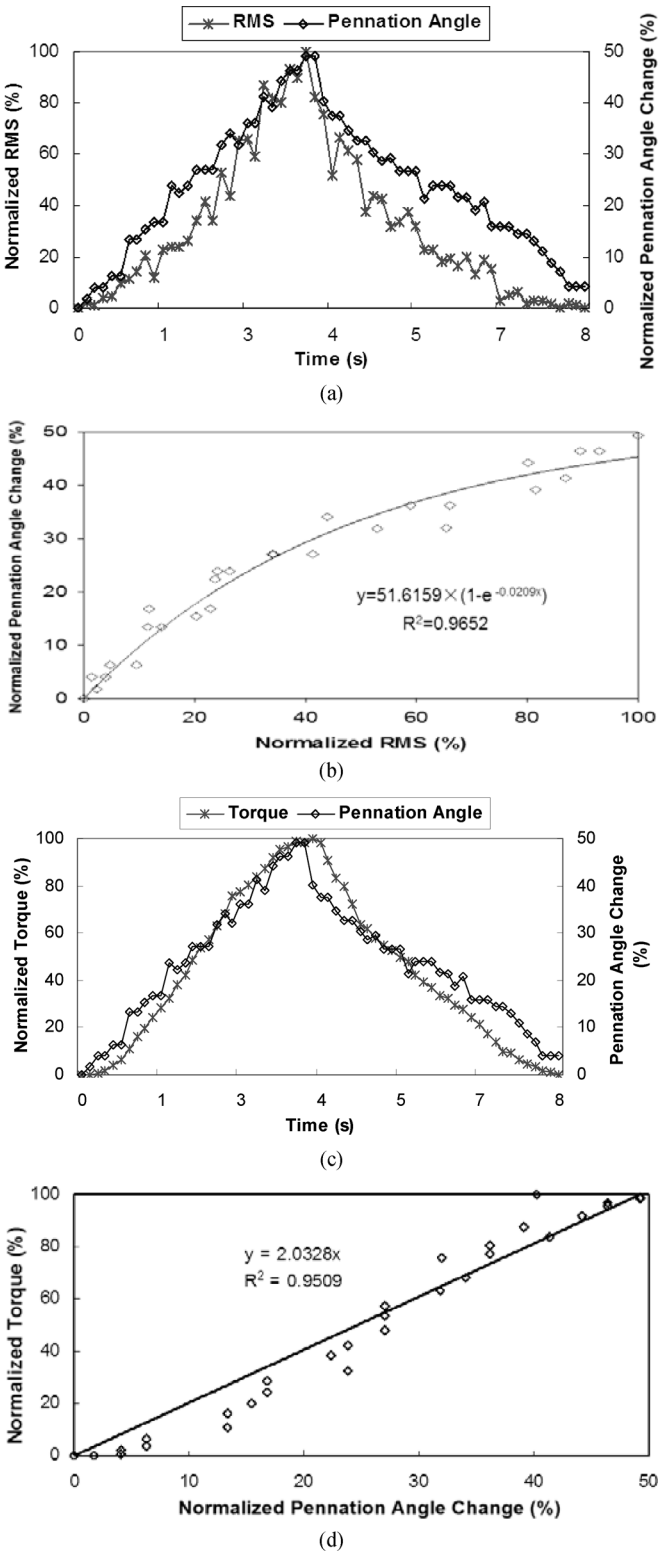

Fig. 5. Typical relationships between the torque, EMG RMS and brachialis pennation angle. (a) The pennation angle and RMS. (b) The exponential regression between the pennation angle and RMS. (c) The torque and pennation angle. (d) The linear regression between the torque and pennation angle.

Our results demonstrated exponential relationships between the EMG RMS and the torque, the RMS and the muscle deformation, and the RMS and the pennation angle for the biceps in the contraction phase. These results were consistent with those previously reported [7], [27], [28]. It was further demonstrated that there was a linear relationship between the torque and the muscle deformation during the contraction phase and a similar linear relationship was found between the torque and the muscle pennation angle change. Our results appeared to imply that there was a better linear relationship between the architectural changes of the muscle and the generated torque, which is related to the muscle force. Further studies with more subjects should be followed to consolidate these findings. Since the muscle fiber length can be derived from the pennation angle, muscle thickness, and location of the aponeurosis shown in the ultrasound image [30], future studies could also be followed to investigate the relationships among the muscle fiber length, torque and parameters of EMG noninvasively.

The relationship between the muscle architectures and its functional capabilities has recently attracted many research efforts [31]. The results of this study appear to imply that the architectural changes during muscle contraction relate more directly to the actuation achieved (mechanical output), while the EMG is a measure of activation intended (electrical input). Similar findings had been reported in a study using SMG for muscle fatigue assessment [32]. The complementary information provided by SMG and EMG may form a comprehensive assessment of muscle contractions. Furthermore, another signal about muscle contraction, named as mechanomyogram (MMG), has also been widely investigated recently. MMS is a measure of vibration of muscle fibers during contraction. Further studies to simultaneously collect EMG, MMG and SMG are currently being conducted. We believe that the combined information can provide a better understanding of muscle contraction mechanism and its relationships with various pathological conditions.

V. Conclusion

We investigated the contractile process of the biceps brachii with continuously sampled ultrasound image, torque, and EMG. The results showed that there were exponential relationships between the torque and the RMS of EMG, and between the RMS and muscle deformation SMG as well as the pennation angle SMG, but a linear relationship between the torque and the muscle deformation as well as the pennation angle change. The underlying mechanism for such relationships requires further investigations. Future studies are also necessary to investigate the parameters obtained in the relaxation phase of the muscle contraction cycles with a higher frame rate for the data collection. Our results suggested that the sonomyography signals, i.e., the muscle deformation and pennation angle change detected using ultrasound, could potentially provide complementary information for the muscle assessment together with the widely used parameters including EMG and torque signals, such as during muscle fatigue analysis, electrical stimulation, and analysis of muscle atrophy.

REFERENCES

[1] A. L. Hof, "EMG and muscle force: An introduction," *Human Movement Sci.*, vol. 3, pp. 119–153, 1984.

[2] A. F. Mannion and P. Dolan, "The effects of muscle length and force output on the EMG power spectrum of the erector spinae," *J. Electromyogr. Kinesiol.*, vol. 6, pp. 159–168, 1996.

[3] M. Naeije and H. Zorn, "Relation between EMG power spectrum shift and muscle-fiber action-potential conduction-velocity changes during local muscular fatigue in man," *Eur. J. Appl. Physiol.*, vol. 50, pp. 23–33, 1982.

[4] D. Farina and R. Merletti, "A novel approach for estimating muscle fiber conduction velocity by spatial and temporal filtering of surface EMG signals," *IEEE Trans. Biomed. Eng.*, vol. 50, pp. 1340–1351, 2003.

[5] M. Pozzo, E. Merlo, D. Farina, G. Antonutto, R. Merletti, and P. D. Prampero, "Muscle-fiber conduction velocity estimated from surface EMG signals during explosive dynamic contractions," *Muscle Nerve*, vol. 29, pp. 823–833, 2004.

[6] G. Misuri, S. Colagrande, M. Gorini, I. Iandelli, M. Mancini, R. Duranti, and G. Scano, "In vivo ultrasound assessment of respiratory function of abdominal muscles in normal subjects," *Eur. Respir. J.*, vol. 10, pp. 2861–2867, 1997.

[7] P. W. Hodges, L. H. M. Pengel, R. D. Herbert, and S. C. Gandevia, "Measurement of muscle contraction with ultrasound imaging," *Muscle Nerve*, vol. 27, pp. 682–692, 2003.

[8] Y. P. Zheng, M. M. F. Chan, J. Shi, X. Chen, and Q. H. Huang, "Sonomyography: Monitoring morphological changes of forearm muscles in actions with the feasibility for the control of powered prosthesis," *Med. Eng. Phys.*, vol. 28, no. 5, pp. 405–415, 2006.

[9] M. V. Narici, T. Binzoni, E. Hiltbrand, J. Fasel, F. Terrier, and P. Cerretelli, "In vivo human gastrocnemius architecture with changing joint angle at rest and during graded isometric contraction," *J. Physiol.*, vol. 496, no. 1, pp. 287–297, 1996.

[10] T. Fukunaga, Y. Ichinose, M. Ito, Y. Kawakami, and S. Fukashiro, "Determination of fascicle length and pennation in a contracting human muscle in vivo," *J. Appl. Physiol.*, vol. 82, pp. 354–358, 1997.

[11] M. Ito, Y. Kawakami, and Y. Ichinose, "Nonisometric behavior of fascicles during isometric contractions of a human muscle," *J. Appl. Physiol.*, vol. 85, pp. 1230–1235, 1998.

[12] C. N. Maganaris, V. Baltzopoulos, and A. J. Sargeant, "Repeated contractions alter the geometry of human skeletal muscle," *J. Appl. Physiol.*, vol. 93, pp. 2089–2094, 2002.

[13] L. Mademli and A. Arampatzis, "Behaviour of the human gastrocnemius muscle architecture during submaximal isometric fatigue," *Eur. J. Appl. Physiol.*, vol. 94, pp. 611–617, 2005.

[14] N. D. Reeves, C. N. Maganaris, and M. V. Narici, "Ultrasonographic assessment of human skeletal muscle size," *Eur. J. Appl. Physiol.*, vol. 91, pp. 116–118, 2004.

[15] C. N. Maganaris, V. Baltzopoulos, and A. J. Sargeant, "Human calf muscle responses during repeated isometric plantarflexions," *J. Biomechan.*, vol. 39, pp. 1249–1255, 2006.

[16] C. Nordander, J. Willner, G. A. Hansson, B. Larsson, J. Unge, L. Granquist, and S. Skerfving, "Influence of the subcutaneous fat layer, as measured by ultrasound, skinfold calipers and BMI, on the EMG amplitude," *Eur. J. Appl. Physiol.*, vol. 89, pp. 514–519, 2003.

[17] J. M. McMeeken, I. D. Beith, and D. J. Newham, "The relationship between EMG and change in thickness of transversus abdominis," *Clin. Biomech.*, vol. 19, pp. 337–342, 2004.

[18] I. Hatta, H. Sugi, and Y. Tamura, "Stiffness changes in frog skeletal muscle during contraction recorded using ultrasonic waves," *J, Physiol.*, vol. 403, pp. 193–209, 1988.

[19] T. Tsuchiya, H. Iwamoto, Y. Tamura, and H. Sugi, "Measurement of transverse stiffness during contraction in frog skeletal muscle using scanning laser acoustic microscope," *Jpn. J. Physiol.*, vol. 43, pp. 649–647, 1993.

[20] J. L. Gennisson, C. Cornu, S. Catheline, M. Fink, and P. Portero, "Human muscle hardness assessment during incremental isometric contraction using transient elastography," *J. Biomech.*, vol. 38, pp. 1543–1550, 2005.

[21] Q. H. Huang, Y. P. Zheng, M. H. Lu, and Z. R. Chi, "Development of a portable 3D ultrasound imaging system for musculoskeletal tissues," *Ultrasonics*, vol. 43, pp. 153–163, 2005.

[22] G. Cao, J. Jiang, and J. Chen, "An improved object tracking algorithm based on image correlation," in *IEEE Int. Symp. Ind. Electron.*, 2004, vol. 1, pp. 598–601.

[23] S. Lou, Q. Zhang, F. Lou, and Y. Wang, "An improved correlation tracking algorithm based on adaptive template modification," in *Proc. 2004 Int. Conf. Information Acquisition*, 2004, pp. 313–315.

[24] D. A. Montera, S. K. Rogers, D. W. Ruck, and M. E. Oxley, "Object tracking through adaptive correlation," *Opt. Eng.*, vol. 33, pp. 294–302, 1994.

[25] R. D. Herbert and S. C. Gandevia, "Changes in pennation with joint angle and muscle torque: In vivo measurements in huam brachialis muscle," *J. Physiol.*, vol. 484, pp. 523–532, 1995.

[26] J. J. Luh, G. C. Chang, C. K. Cheng, J. S. Lai, and e.-S. Kuo, "Isokinetic elbow joint torques estimation from surface EMG and joint kinematic data: Using an artificial neural network model," *J. Electromyogr. Kinesiol.*, vol. 9, pp. 173–183, 1999.

[27] J. V. Basmajian and C. J. De Luca, *Muscles Alive: Their Functions Revealed by Electromyography*, 5th ed. Baltimore, MD: Williams & Wilkins, 1985.

[28] C. J. DeLuca, "The use of surface electromyography in biomechanics," *J. Appl. Biomech.*, vol. 13, pp. 135–163, 1997.

[29] C. Orizio, M. Gobbo, A. Veicsteinas, R. V. Baratta, B. H. Zhou, and M. Solomonow, *Eur. J. Appl. Physiol.*, vol. 88, pp. 601–606, 2003.

[30] T. Finni and P. V. Komi, "Two methods for estimating tendinous tissue elongation during human movement," *J. Appl. Biomech.*, vol. 18, pp. 180–188, 2002.

[31] B. J. J. J. Van der Linden, H. F. J. M. Koopman, H. J. Grootenboer, and P. A. Huijing, "Modelling functional effects of muscle geometry," *J Electromyogr. Kinesiol.*, vol. 8, pp. 101–109, 1998.

[32] J. Shi, Y. P. Zheng, X. Chen, and Q. H. Huang, "Assessment of muscle fatigue using sonomyography: Muscle thickness change detected from ultrasound images," *Med. Eng. Phys.*, vol. 29, pp. 472–479, 2007.

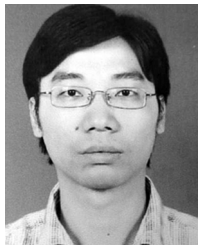

Jun Shi received the B.S. degree from the Department of Electronic Engineering and Information Science, University of Science and Technology of China, in 2000. He received the Ph.D. degree from the same university in 2005.

During his graduate studies, he worked as a Research Assistant in the group of Dr. Y.-P. Zheng in the Jockey Club Rehabilitation Engineering Centre at the Hong Kong Polytechnic University from 2002 to 2003. In 2005, he joined the School of Communication and Information Engineering at Shanghai University as a Lecturer. His research interests include ultrasound signal processing, medical instrument development, ultrasound applications for elastography, musculoskeletal tissues, and acoustic microscopes.

Yong-Ping Zheng (S'95–A'98–M'99–SM'06) received the B.Sc. degree in electronics and information engineering and the M.Eng. degree in ultrasound instrumentation from the University of Science and Technology of China, Hefei. He received the Ph.D. degree in biomedical engineering from the Hong Kong Polytechnic University (PolyU), Hong Kong, in 1997.

After a postdoctoral fellowship in acoustic microscope and nonlinear acoustics at the University of Windsor, Windsor, ON, Canada, he joined PolyU as an Assistant Professor in 2001 and became an Associate Professor in 2005. His main research interests include ultrasound elasticity imaging and measurement, three-dimensional ultrasound imaging, ultrasonic characterization of muscle and articular cartilage, and ultrasound instrumentation. He and his co-workers hold four U.S. patents, and have nine patents filed in the U.S. and China since 2002, mainly in the field of biomedical ultrasound.

Qing-Hua Huang (S'05–M'06) was born in Heilongjiang, China, in November 1976. He received the B.E. degree in automatic control and the M.E. degree in pattern recognition, both from the University of Science and Technology of China, Hefei, in 1999 and 2002. He received the Ph.D. degree in biomedical engineering in July 2006 from the Hong Kong Polytechnic University (PolyU).

He joined the Rehabilitation Engineering Center of PolyU as a Research Assistant in 2002, and was a Research Associate with the Department of Health Technology and Informatics at the same university in 2006. He is now a Postdoctoral Research Fellow in the Department of Electronic Engineering, City University of Hong Kong. His research interests include three-dimensional ultrasound imaging, medical image analysis, and intelligent computation for biomedical signals and bioinformatics.

Xin Chen received the Ph.D. degree in biomedical engineering from the University of Science and Technology of China, Hefei, in 2003.

He held the position of Research Associate at the Hong Kong Polytechnic University, Hong Kong, since 2003. He is currently with the Department of Health Technology and Informatics of the same university. His primary research interests include biomedical ultrasound instrumentation, ultrasonic measurement and imaging of tissue elasticity, and ultrasound assessment of musculoskeletal tissues.